

PCCP

Accepted Manuscript



This is an *Accepted Manuscript*, which has been through the Royal Society of Chemistry peer review process and has been accepted for publication.

Accepted Manuscripts are published online shortly after acceptance, before technical editing, formatting and proof reading. Using this free service, authors can make their results available to the community, in citable form, before we publish the edited article. We will replace this *Accepted Manuscript* with the edited and formatted *Advance Article* as soon as it is available.

You can find more information about *Accepted Manuscripts* in the [Information for Authors](#).

Please note that technical editing may introduce minor changes to the text and/or graphics, which may alter content. The journal's standard [Terms & Conditions](#) and the [Ethical guidelines](#) still apply. In no event shall the Royal Society of Chemistry be held responsible for any errors or omissions in this *Accepted Manuscript* or any consequences arising from the use of any information it contains.

Specific Adsorption of Perchlorate Anions on Pt{*hkl*} Single Crystal Electrodes

Gary A. Attard^{1,*}, Ashley Brew¹, Katherine Hunter¹, Jonathan Sharman² and Edward Wright²

¹Cardiff Catalysis Institute, School of Chemistry, Cardiff University, Cardiff CF10 3AT, UK

²Johnson Matthey Technology Centre, Blounts Court Road, Sonning Common, Reading, Berkshire, RG4 9NH, UK

*To whom correspondence should be addressed

e-mail: attard@cardiff.ac.uk

Tel. +44(0)2920 874069

Fax. +44(0)2920 874030

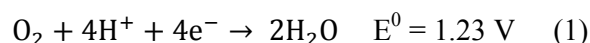
Abstract

The voltammetry of Pt{111}, Pt{100}, Pt{110} and Pt{311} single crystal electrodes as a function of perchloric acid concentration (0.05 – 2.00 M) has been studied in order to test the assertion made in recent reports by Watanabe *et al.* that perchlorate anions specifically adsorb on polycrystalline platinum. Such an assertion would have significant ramifications for our understanding of electrocatalytic processes at platinum surfaces since perchlorate anions at low pH have classically been assumed not to specifically adsorb. For Pt{111}, it is found that OH_{ad} and electrochemical oxide states are both perturbed significantly as perchloric acid concentration is increased. We suggest that this is due to specific adsorption of perchlorate anions competing with OH_{ad} for adsorption sites. The hydrogen underpotential deposition (H UPD) region of Pt{111} however remains unchanged although evidence for perchlorate anion decomposition to chloride on Pt{111} is reported. In contrast, for Pt{100} no variation in the onset of electrochemical oxide formation is found nor any shift in the potential of the OH_{ad} state which normally results from the action of specifically adsorbing anions. This suggests that perchlorate anions are non-specifically adsorbed on this plane although strong changes in all H UPD states are observed as perchloric acid concentration is increased. This manifests itself as a redistribution of charge from the H UPD state situated at more positive potential to the one at more negative potential. For Pt{110} and Pt{311}, marginal changes in the onset of electrochemical oxide formation are recorded, associated with specific adsorption of perchlorate. Specific adsorption of perchlorate anions on Pt{111} is deleterious to electrocatalytic activity in relation to the oxygen reduction reaction (ORR) as measured

using a rotating disc electrode (RDE) in a hanging meniscus configuration. This study supports previous work suggesting that a large component of the ORR activity on platinum is governed by simple site blocking by specifically adsorbed anions and/or electroadsorbed oxide.

1. Introduction

The need to move away from purely fossil fuel based transport modalities (due to resource limitations, legislative imperatives and environmental issues) is re-focussing research efforts towards the development of new approaches based on biofuels and electric/hybrid vehicles including Battery Electric Vehicles and Fuel Cell Electric Vehicles (FCEVs)¹⁻⁵. Although each of these avenues offers a partial solution towards an overall energy efficient transport strategy, each has its drawbacks therefore inhibiting any one approach from commanding overall commercial acceptance. These issues are the focus of a great deal of current work^{4,8}. Fuel cell technology for example has the potential to find use in many applications of varying scale, from small mobile devices to large transport vehicles. However, large scale utilisation of FCEVs is hindered by a number of factors - the price of the vehicles themselves due to the expense of both the platinum electrocatalyst together with the engineering constraints associated with membrane, support and catalyst stability^{3,4}, the infrastructure required for hydrogen-fuelled FCEVs is poorly developed and would require significant investment (and public confidence) before becoming economically viable and finally, fundamentally, the relatively poor electrocatalytic activity of even the best ORR electrocatalysts currently in use today. Hence, a significant scientific and engineering challenge remains before full implementation of fuel cell technology can be considered successful. In this context, we present some new results pertaining to the problem of electrocatalysis using platinum. At the cathode of a FCEV, the oxygen reduction reaction (ORR) proceeds. The complete reaction involves the 4 electron reduction of oxygen to water molecules according to equation 1.



The corresponding anodic reaction in the Proton Exchange Membrane Fuel Cell (PEMFC) is the oxidation of hydrogen to protons according to equation 2.



The hydrogen oxidation reaction (HOR) is facile over a platinum catalyst whereas the ORR requires a large overpotential, and therefore a large amount of expensive platinum electrocatalyst, to run at an appreciable rate. This constitutes the major bottleneck in fuel cell technology. Understanding the origin of the overpotential for the oxygen reduction reaction

(ORR) on real platinum nanoparticle surfaces would represent a crucial advance in our fundamental knowledge and this problem lies at the heart of much scientific endeavour^{6, 9-14}. Since the composition and structure of the electrocatalyst surface are paramount in relation to many electrocatalytic reactions, especially the ORR¹⁰⁻²⁴ much work has been carried out using single crystal electrode surfaces in order to simplify the problem^{11-13, 15-17}. Exposing only a specific electrode surface with the desired atomic arrangement to an electrolyte enables structure-activity relationships to be obtained between the adsorbate and electrochemical reactions under investigation and thus may direct synthesis of “shape-controlled” nanoparticles for optimal electrocatalytic performance^{24, 25}. Early work used single crystals to study the ORR over the basal planes of platinum¹⁵⁻¹⁷. In these studies it was shown that in sulphuric acid electrolyte the activity was relatively low due to the strong specific adsorption of bisulphate ions which block O₂ adsorption and its’ subsequent reduction at more negative potentials^{15, 24, 26, 27}. In fact, strongly adsorbed ions and impurities often facilitated the two electron reduction of oxygen to hydrogen peroxide on platinum electrodes^{28, 29}. A higher activity for ORR of stepped Pt{111} surfaces in sulphuric acid electrolyte relative to the Pt{111} plane itself has been attributed to the breaking up of an ordered sulphate/bisulphate adlayer formed on Pt{111} at potentials commensurate with the on-set of ORR, thus facilitating greater O₂ adsorption and dissociation due to decreased competition for metallic platinum adsorption sites^{11, 12}.

In order to understand the ORR mechanism in the absence of such anion adsorption effects, investigations have also been carried out using perchloric acid, an electrolyte widely considered to exhibit zero or negligible specific adsorption of ClO₄⁻ upon Pt{hkl} surfaces^{11, 12, 30-34}. However, recent papers by Watanabe and co-workers using CV, in situ infra-red and quartz crystal microbalance measurements have demonstrated on polycrystalline platinum electrodes that perchlorate anions may specifically adsorb and moreover as a consequence inhibit ORR due to introducing a potentially site-blocking specifically adsorbing anion which competes successfully for adsorption sites with O₂^{35, 36}. Since it is already well-known that single crystal platinum electrode voltammetry is highly sensitive to specific adsorption, it was thought prudent to test the notion of perchlorate specific adsorption using Pt{hkl} since the effect should be much more prominent compared to polycrystalline substrates³⁵. When electrosorption peaks do not overlap with specific adsorption processes (as is found for hydrogen underpotential deposition (H UPD) states on Pt{111} electrodes in acidic media for example), no perturbation of these states is observed when switching from non-specific to specific anion containing aqueous media. However, for states corresponding to OH_{ad}

formation on Pt{hkl}, such electroadsorption peaks are strongly modified by specific adsorption, the paradigmatic system to show this effect usually being the comparison between cyclic voltammograms of a particular Pt{hkl} electrode obtained in aqueous perchloric or sulphuric acid^{26, 27, 37-42}. Specific adsorption of anions may also increase the onset potential for electrochemical oxide formation, again presumably due to competition for adsorption sites between the anion and water dissociation pathways. Hence, the extent of specific adsorption should also be reflected in the shift in potential for the formation of electroadsorbed oxide. The activity towards ORR of basal plane and stepped platinum surfaces is strongly attenuated as electroadsorbed oxide is formed since O₂ adsorption and dissociation is facilitated at metallic sites^{11, 12, 17}. Hence, both oxide formation and specific adsorption of anions are found to inhibit ORR activity. Recent work has demonstrated that optimisation of adsorbate-substrate interactions (using the Sabatier principle) is also crucial in optimising ORR activity^{6, 14, 43, 44} with a number of bimetallic platinum alloy electrodes affording superior activity to platinum in this regard^{14, 20, 45} although electrocatalyst stability remains a challenging problem^{46, 47}.

Considering the fact that ClO₄⁻ is known to adsorb (and decompose) at a number of metal electrode surfaces (including Rh, Ir, Ru and Pd)⁴⁸⁻⁵², it is important to consider the possibility that ClO₄⁻ in acidic aqueous media may have more of a role to play in the electrooxidation of platinum surfaces and also in electrocatalytic reactions such as oxygen reduction. This view contrasts with the role of spectator that this anion currently is thought to hold in most interpretations of platinum electrocatalytic research. In the present study, we shall explore the case for specific adsorption of ClO₄⁻ in perchloric acid electrolyte (as reported by Watanabe et al.^{35, 36}) by employing cyclic voltammetry studies of Pt{hkl} electrodes. The impact that this anion may have on the ORR in relation to Nafion[®] adsorption and other specifically adsorbing species on Pt{111} electrodes will also be discussed.

2. Experimental

HClO₄ (70% Suprapur[®] supplied by Merck), NaOH (Sigma-Aldrich ≥99.9995%), H₂SO₄ (Aristar 95%) and HCl (Fischer Chemical ~37.5%) were used to prepare all aqueous electrolyte solutions (Millipore ultra-pure water, resistivity >18.2 MΩ·cm). Platinum single crystal electrodes, typically 2 – 3 mm in diameter were prepared using the method of Clavilier⁵³. The electrochemical cell, palladium-hydrogen reference electrode and apparatus for recording voltammetric data have all been described previously⁵⁴. A palladium hydride

reference electrode was used for HClO₄, H₂SO₄ and HCl electrolytes and a Ag/AgCl_(sat) reference electrode was used when collecting the aqueous NaOH data. However, all potentials are reported with reference to the palladium hydride reference electrode contained within the electrolyte.

ORR measurements were collected using a Basi RDE-2 rotating disc electrode system controlling the hydrodynamics of the reaction in the hanging meniscus configuration⁵⁵. The cell used for RDE measurements also contained a Pd/H reference electrode within a luggin capillary containing degassed aqueous electrolyte. Oxygen of purity 99.999% from BOC was bubbled through the RDE electrochemical cell for 30 minutes prior to performing any ORR measurement. After saturating the electrolyte with oxygen, bubbling into the electrolyte was discontinued and a positive pressure of oxygen was maintained across the electrolyte during all ORR measurements. All CV data employed a potential sweep rate of 50 mV/s unless stated otherwise. Surface characterisation of the single crystal electrodes was performed via CV in various electrolytes (all electrolytes having been degassed in the electrochemical cell for at least 30 minutes with nitrogen gas prior to any CV measurement). After flame-annealing the electrode and cooling in a stream of hydrogen-saturated water vapour, the electrode was transferred to the electrochemical cell and a meniscus contact was formed. The method of forming a clean, Nafion adlayer upon a Pt{111} single crystal electrode has also been described previously^{56,57} and was used without change in the present study. The ORR activity of Pt{111} single crystal surfaces was measured by potential controlled contact with the electrolyte at 0 V, before applying a linear, positive potential sweep of 30mV/s up to 1 V versus Pd/H in order to exclude possible structural perturbations associated with the rather positive open circuit potential corresponding to oxygen saturated electrolyte.

3. Results and Discussion

3.1 Cyclic voltammetry of Pt{hkl} as a function of perchloric acid concentration

3.1.1 Pt{111}

Figure 1 shows CV data collected using a Pt{111} electrode as a function of increasing aqueous perchloric acid concentration. The CV responses are typical of a well-ordered Pt{111} electrode in this electrolyte showing a clear separation between H UPD (0 - 0.3 V), OH_{ad} (0.5 – 0.8 V) and electrochemical oxide (0.95 – 1.1 V) states^{31,58}. For the H UPD electrosorption peaks, there is no impact either upon the magnitude or distribution of electrosorption charge as acid concentration is increased. This suggests that the strength of

perchlorate anion adsorption (if occurring) is insufficient to perturb these adsorption states. In contrast, both the OH_{ad} and electrochemical oxide peaks show modifications in their shape and magnitude. The electrochemical oxide peak in particular is observed to shift from 0.98 V (0.05 M) to 1.03 V (2.0 M) with a corresponding increase in intensity and narrowing in half-width. This behaviour would be consistent with the presence of a specifically adsorbing anion competing successfully for adsorption sites with water splitting pathways. In fact this point is also reflected in the marked attenuation in the broader component of the so-called “butterfly” peak and a diminution in the magnitude of the narrower spike which also shifts to more positive potentials as acid concentration is increased. Both of these components of the butterfly peak have been ascribed to reaction of two types of water with the $\text{Pt}\{111\}$ plane to form OH_{ad} ⁵⁹.

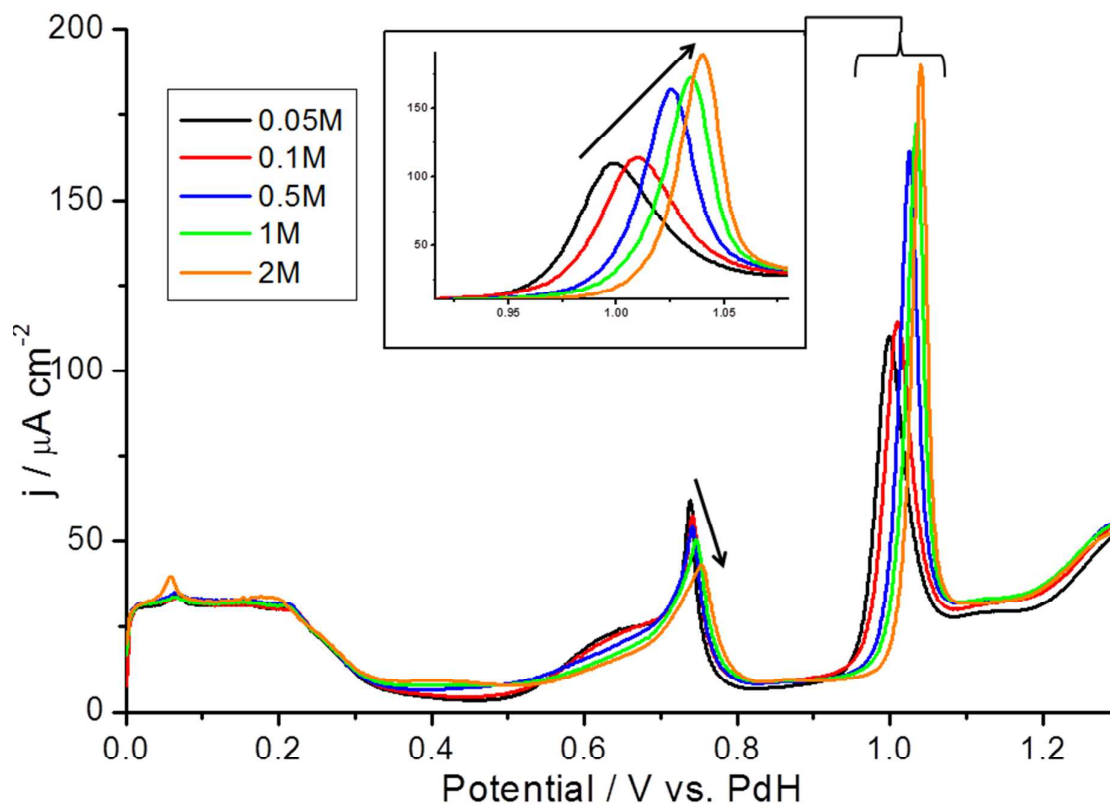


Figure 1 CV data for $\text{Pt}\{111\}$ as a function of aqueous perchloric acid concentration. Sweep rate = 50 mV/s.

In figure 2 (a) we try to mimic this effect by adding small amounts of sulphuric acid to the perchloric acid electrolyte since sulphate is known to specifically adsorb on $\text{Pt}\{111\}$. It is

evident from figure 2 (a) that the changes outlined in figure 1 in relation to OH_{ad} are also observed in figure 2 (a) as exemplified by the shift to more positive potentials of the spike and quenching of the broad peak situated at more negative potentials. Of course a new state begins to appear between 0.4 and 0.6 V corresponding to the specific adsorption of sulphate anions³¹. The asymmetry in this feature at concentrations of sulphuric acid less than approximately 10^{-4} M are associated with mass transport effects⁵⁹. Nonetheless, it is clear that when both OH_{ad} and electrochemical oxide formation states are taken together, it suggests strongly that there is a specifically adsorbing anion present. Since perchlorate anions are known to be electrochemically reduced to chloride on some transition metal surfaces⁵², measurements of perchloric acid deliberately spiked with chloride were also taken in order to eliminate the possibility of the strongly adsorbing chloride anion being responsible for the behaviour reported above.

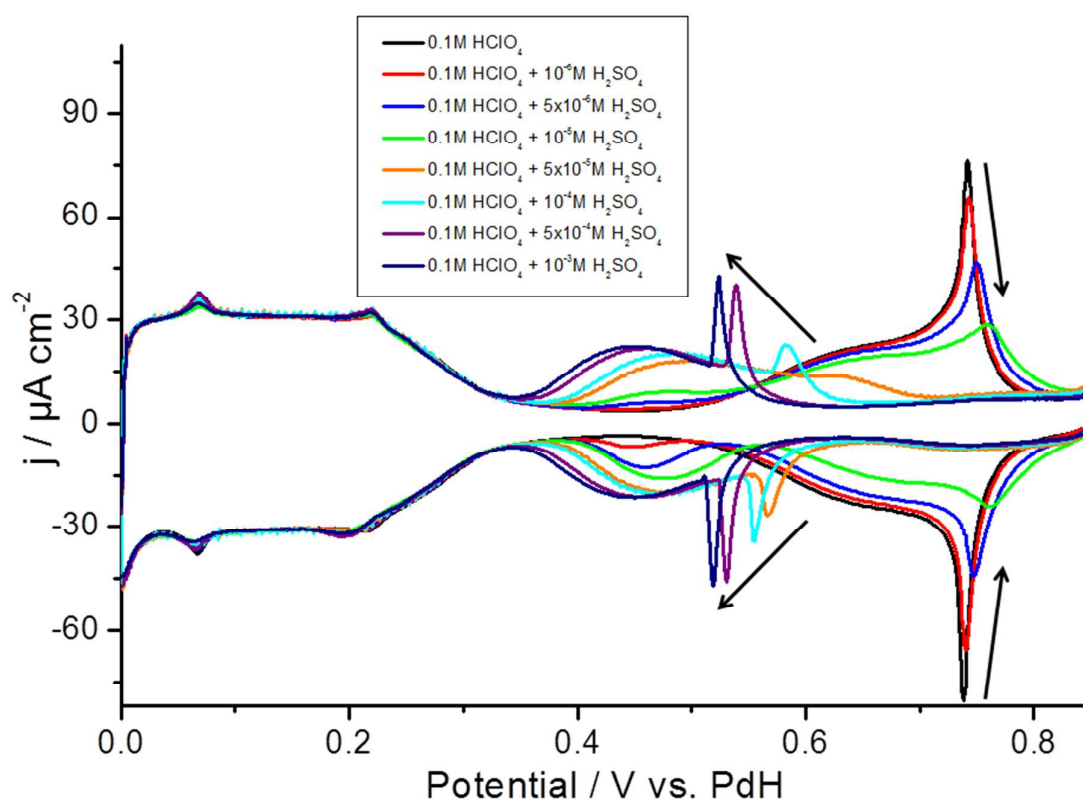


Figure 2 (a) CV data for Pt{111} in 0.1 M aqueous perchloric acid as a function of increasing sulphuric acid concentration. Sweep rate = 50 mV/s.

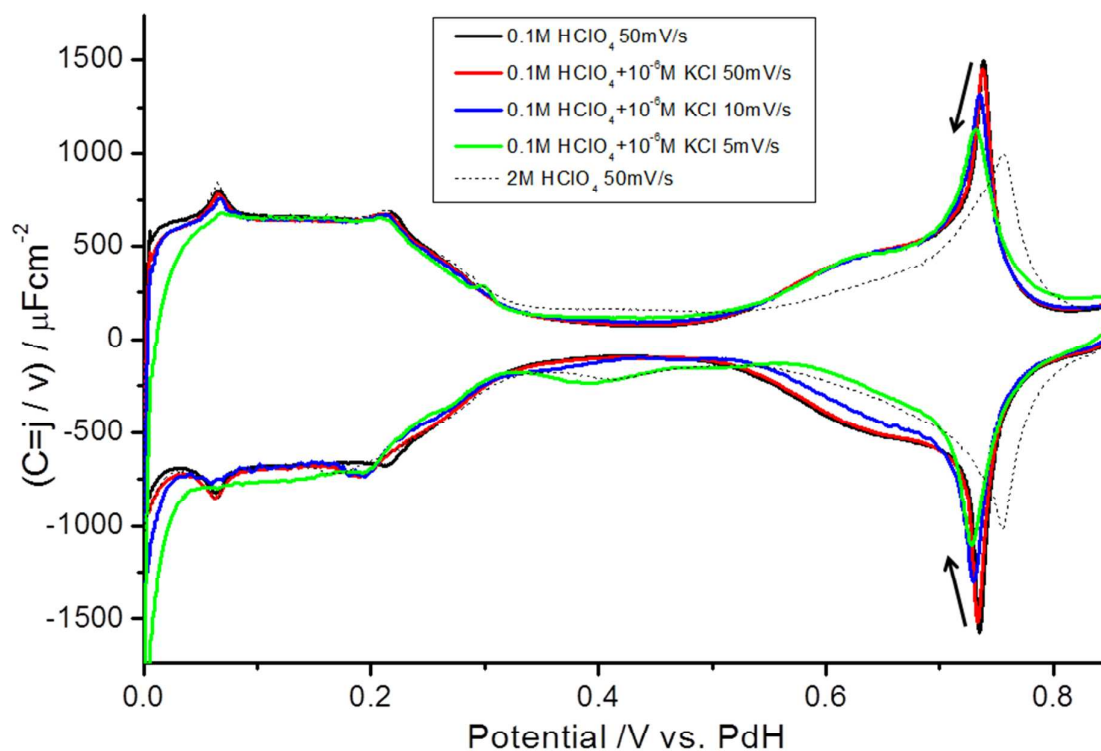


Figure 2 (b) Capacitance (current density/sweep rate) versus potential for Pt{111} in 0.1 M perchloric acid as a function of uptake of chloride anions. The dotted curve refers to data collected in 2 M aqueous perchloric acid.

Figure 2 (b) shows data for 0.1 M perchloric acid with 10^{-6} M chloride added as a function of potential sweep rate. Since adsorption of chloride was being determined by mass transport limitations under these conditions, it was possible, by slowing down the sweep rate of the CV, to afford larger and larger degrees of chloride coverage. On the positive going sweep, the effect of chloride is hardly observed for the broad butterfly peak component but in contrast, the spike systematically shifts to more negative potentials (in contrast to sulphate). This behaviour has already been reported by Berna et al⁵⁹. On the negative going sweep, because the time spent at the more positive potential is greatest, it allows more time for chloride to adsorb (this is also true of the sulphate peaks in figure 2 (a) whereby a higher intensity was seen on the negative going sweep). As a consequence, the broad butterfly peak feature begins to be attenuated since adsorbed chloride has blocked OH_{ad} sites and in addition, a new peak is observed in the 5 mV/s scan ascribable to specific adsorption of chloride at 0.4 V. The dotted curve in this figure is the superposition of the Pt{111} CV collected in 2 M

aqueous perchloric acid. It is evident that an extra peak in this CV upon sweeping negative from 0.85 V is observed at precisely the potential associated with specifically adsorbed chloride. Hence, could this be evidence of chloride contamination in the 2 M perchloric acid? We suggest not. When chloride is actually present as an impurity in the electrolyte, it manifests itself as both a blocking of the OH_{ad} states in the broad butterfly peak feature and a shift to negative potentials in the spike. Yet in 2 M perchloric acid, the spike shifts positively from its position in 0.1 M perchloric acid (like sulphate). Moreover, we shall see later that chloride cannot be present in the electrolyte based on the CV response of Pt{100} in particular. Therefore, from where could the chloride anion be originating? We suggest that Pt{111} slowly catalyses the reduction of perchlorate anions at potentials commensurate with the beginning of the H UPD region and the double layer as found on Rh, Ir and Pd^{49, 50, 52} and indeed polycrystalline Pt⁴⁸. On Pt{111}, the degree of perchlorate adsorption is extremely small in 0.1 M perchloric acid and hence, only after a x20 increase in perchlorate concentration is this weak effect observed. Evidently, specific adsorption of perchlorate (unlike for bisulphate and dihydrogen phosphate which are isoelectronic with perchlorate) leads to an unstable adsorbed species that decomposes to give chloride anions. The mechanism and kinetics of perchlorate electroreduction have been thoroughly reviewed by Horanyi et al^{36, 49, 52} and in particular, the reduction may even be observed by CV at platinised Pt electrodes at slow sweep rates (1 mV/s) and/or temperatures greater than 298 K⁴⁸. It should be mentioned also that spectroscopic evidence for the specific adsorption of perchlorate on Pt{111} was also first reported by Ito et al^{60, 61}.

3.1.2 Pt{100}

Figure 3 shows changes in the voltammetric behaviour (positive going sweep) of Pt{100} as a function of increasing perchloric acid concentration. The sweep corresponding to 0.1 M electrolyte is typical of a well-ordered Pt{100} electrode and, as for Pt{111}, may be delineated into various regions according to the nature of the electroadsorption processes occurring. From 0 to 0.1 V, the oxidation of hydrogen gas formed in the previous negative going sweep is recorded^{62, 63}. Between 0.1 and 0.4 V broadly corresponds to H UPD processes although these are overlapped by a broad feature extending to about 0.6V that is associated with OH_{ad} on Pt{100}⁶⁴. Finally, at potentials greater than 0.8 V, electrochemical oxidation of the Pt{100} surface takes place leading to the formation of platinum oxide

species^{62, 63}. The H UPD region of Pt{100} in 0.1 M perchloric acid is noteworthy because it actually consists of two states at approximately 0.3 and 0.4 V. Hence, the potential region 0.1 – 0.6 V on Pt{100} contrasts quite markedly with Pt{111} since it comprises a series of overlapping electroadsorption states.

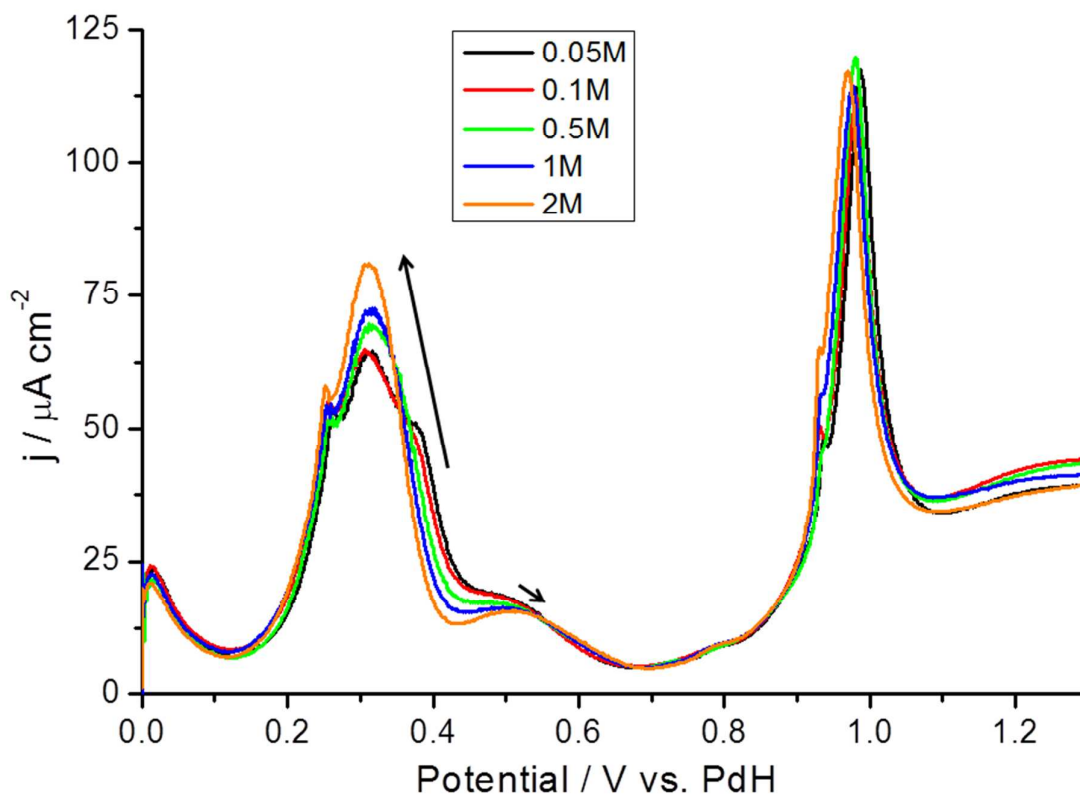


Figure 3 CV data for Pt{100} as a function of aqueous perchloric acid concentration. Sweep rate = 50 mV/s.

The first noteworthy feature of figure 3 compared to figure 1 is that there is hardly any variation at all in either the onset of platinum oxide formation nor in the potential of the platinum oxide peak itself, irrespective of perchloric acid concentration. Furthermore, although there are clearly redistributions of charge from the H UPD state at 0.4 V to that at 0.3 V as acid concentration increases, there is no effect on the OH_{ad} state at 0.5 V. Hence, there appears to be somewhat contradictory behaviour so far as the possibility of specific adsorption is concerned. The electrochemical oxide and OH_{ad} states of Pt{100} do not appear to be affected by the increase in perchlorate concentration consistent with non-specifically adsorbing anion behaviour. In contrast, a shift of H UPD charge from more positive to more

negative potentials as a function of increasing anion concentration is usually a sign of strong specific adsorption with the extent of this shift dependent on the strength of interaction of the anion with the electrode surface⁶³. In order to clarify the influence of specific adsorption on Pt{100} electrosorption peaks, solutions of 0.1 M perchloric acid deliberately spiked with small amounts of sulphate were investigated as electrolytes for Pt{100} (figure 4 (a)). From figure 4 (a) the effect of specific adsorption of sulphate anions results in both a shift to more positive potentials of the OH_{ad} peak at 0.5 V and a displacement of H UPD charge from positive to more negative potentials resulting in a new, sharper peak at 0.36 V associated with H UPD and sulphate adsorption on Pt{100} extended (1x1) terraces^{63, 65}. However, it should be noted that the strength of specific adsorption of sulphate is *insufficient* to displace this new sulphate-induced underpotential deposition peak to 0.3 V (the original value of the H UPD state at most negative potentials on Pt{100}). In fact, the intensity of the original, lower potential H UPD state remains essentially unchanged with the addition of small amounts of sulphuric acid to the 0.1 M perchloric acid electrolyte. Since even sulphate cannot displace the H UPD electrosorption charge into the 0.3 V peak, it is clear that the influence of pH rather than perchlorate anion concentration is the key factor in controlling the relative populations of the two H UPD states on Pt{100} with the state at most negative potential being favoured at low pH and the state at higher potential being preferred at higher pH.

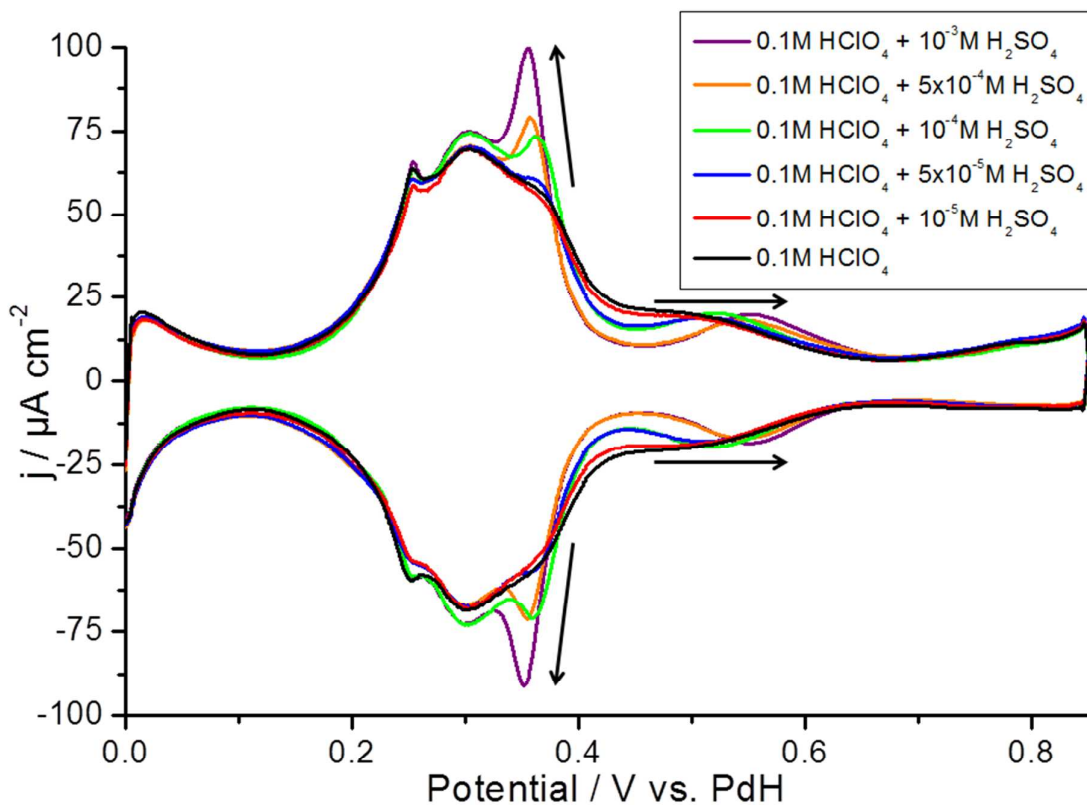


Figure 4 (a) CV data for Pt{100} in 0.1 M aqueous perchloric acid as a function of increasing sulphuric acid concentration. Arrows indicate directions of peak shifts as sulphuric acid concentration increases. Sweep rate = 50 mV/s.

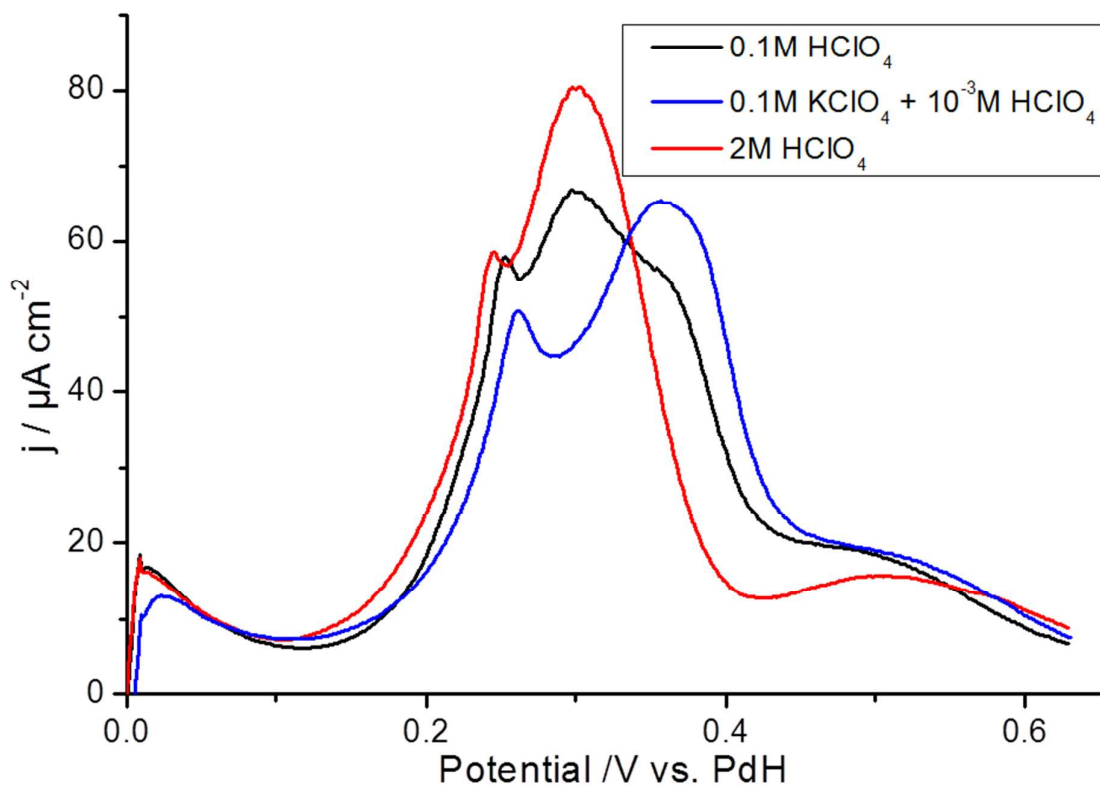


Figure 4 (b) CV data for Pt{100} as a function of aqueous perchloric acid concentration and pH. Sweep rate = 50 mV/s.

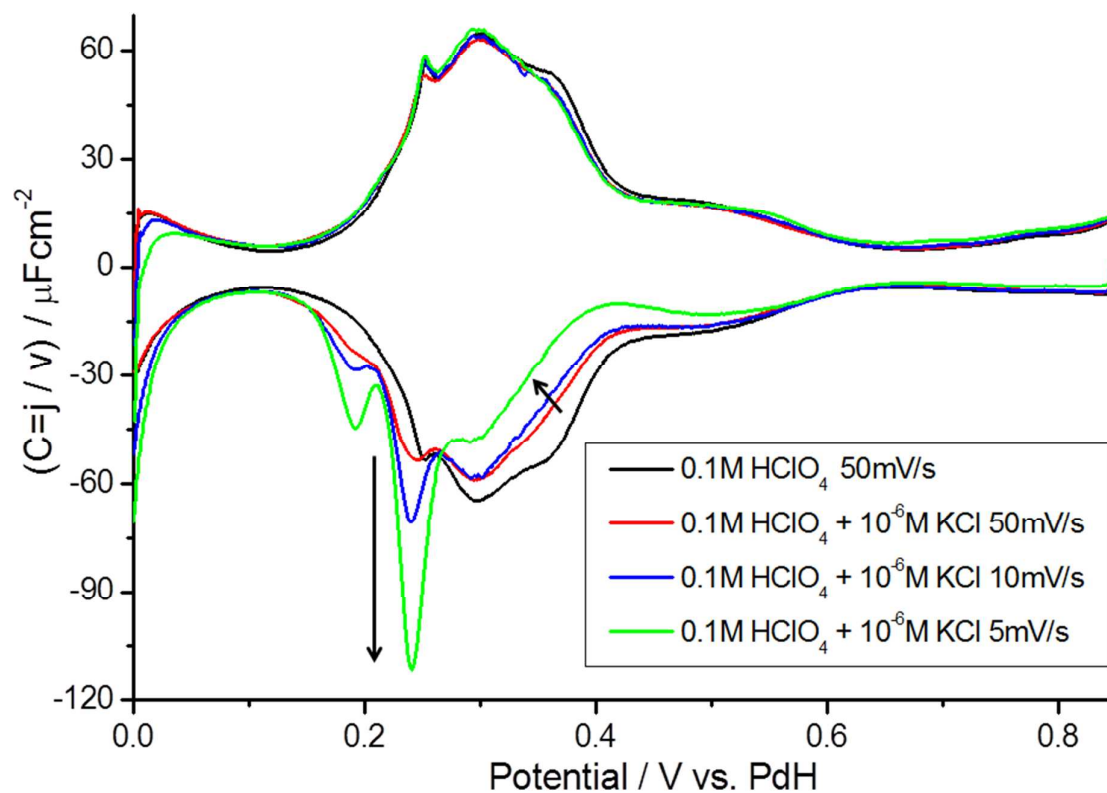


Figure 4 (c) Capacitance (current density/sweep rate) versus potential for Pt{100} in 0.1 M perchloric acid as a function of uptake of chloride anions.

To test this hypothesis, an electrolyte containing 10^{-3} M perchloric acid in 0.1 M KClO_4 was examined. Inspection of figure 4 (b) confirms that the occupation of sites corresponding to the 0.4 V state are favoured at higher pHs and in fact an isobestic point is observed at 0.33 V between the two peaks. The result at pH = 3 was also obtained in reference⁶⁶. It may well be that such behaviour may reflect changes in both adsorption energy and the stability of different adsorbate configurations as noted in reference⁶⁷. Finally, figure 4 (c) shows the effect of chloride on the voltammetry of Pt{100} in perchloric acid (as previously discussed in figure 2 (b) in relation to Pt{111}). On the positive going sweep, there is hardly any perturbation of the CV obtained in 0.1 M perchloric acid irrespective of potential sweep rate. It should be noted that at 10^{-6} M chloride, the CV profile on the positive going sweep bears no relationship to that of Pt{100} in 2 M perchloric acid (figure 3) attesting to the fact that the possibility of contamination by chloride anions is negligible. Upon engaging the reverse sweep however, significant changes in the H UPD states (though not OH_{ad}) are engendered with features negative of 0.3 V consistent with specific adsorption of chloride anions starting

to appear as sweep rate is reduced. The large negative shift in H UPD charge relative to sulphate behaviour is due to chloride's stronger interaction with the platinum surface. Taking all of the results of figures 3 and 4 together, it is evident that specific adsorption of perchlorate anions cannot explain all of the changes described. Rather, pH dependent occupation of H UPD states appears to interpret the data most satisfactorily, especially the lack of perturbation of OH_{ad} and electrochemical oxide peaks as perchloric acid concentration is increased.

3.1.3 Pt{110}

Figures 5 and 6 show how both changes in pH and perchlorate anion concentration influence the CV profile obtained using Pt{110} electrodes. In 0.1 M perchloric acid, the H UPD region consists of two states at 0.09 V and 0.22 V. As found for Pt{100}, strong changes in the relative intensities of both states as a function of pH are observed. However, in contrast to Pt{100}, there are also marked changes in the potential of these H UPD states as a function of pH. For the peak at 0.09 V, a very small shift of potential is seen going from pH = -0.3 to pH = 1 but a shift of 21 mV/pH is observed going from pH = 1 to pH = 3. This non-linear variation with pH over the pH range -0.3 to 3 is somewhat unusual, especially when one realises that a Pd/H reference electrode is being used (if the peak corresponds solely to $\text{H}^+(\text{aq}) + \text{e} = \text{H}_{\text{ads}}$ then no shift should occur whatsoever relative to a Pd/H reference electrode contained within the electrolyte). Hence, at low pH this adsorption state does seem to conform to expectations corresponding to electron transfer consistent with the reduction of protons whereas at higher pH, other processes may be occurring. Detailed discussion of such behaviour for step sites on Pt has recently been published by Koper et al⁶⁸ whereby rationalisation of step peak shifts as a function of pH is found by having various amounts of hydrogen and water at steps being replaced by OH_{ad} and O_{ad} species. For the H UPD peak at 0.22 V, the shift in peak potential is constant over the pH range -0.3 to 1 at 37 mV/pH but shifts by only 15 mV/pH in the range 1 - 3. Hence, the hypothesis that OH-type species may be involved also in the H UPD process associated with the CV peak at 0.22 V is consistent with its pH dependence versus a Pd/H reference electrode. It is also evident from figure 5 that there is a 1:1 correspondence between the attenuation in the intensity of the 0.22 V H UPD peak and growth in the intensity of the 0.09 V peak, similar to what was observed with Pt{100}, as perchloric acid concentration was increased.

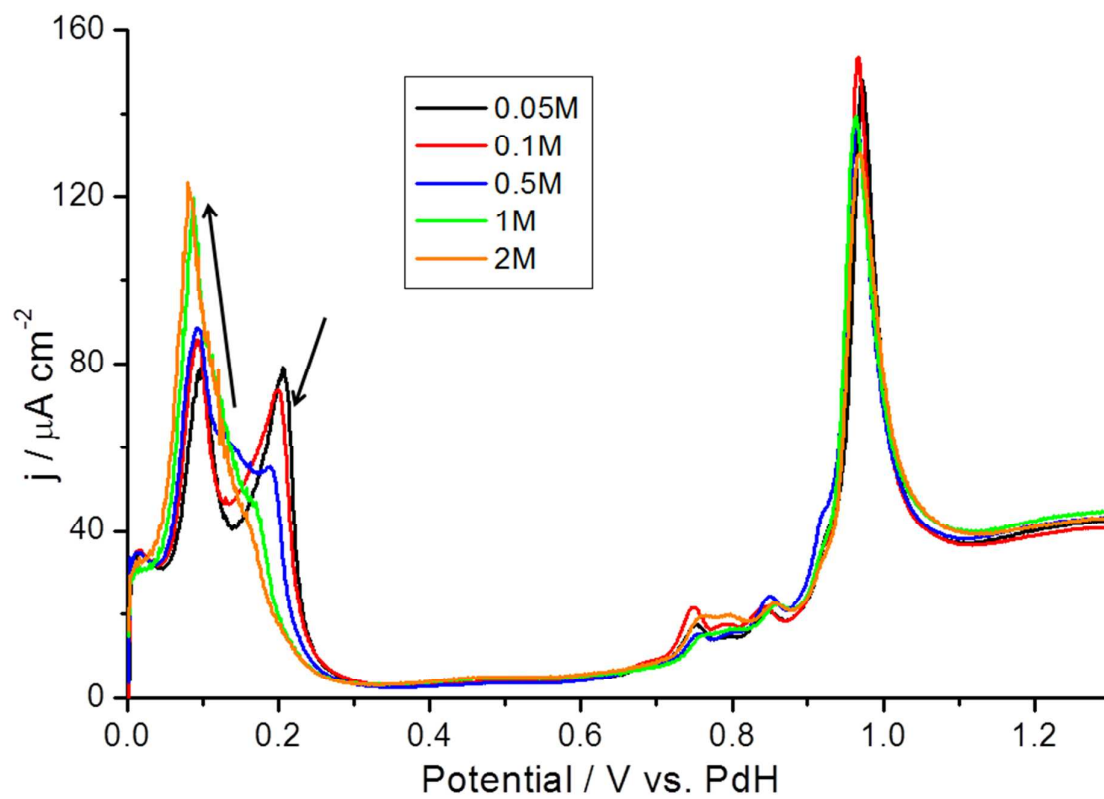


Figure 5 CV data for Pt{110} as a function of aqueous perchloric acid concentration. Sweep rate = 50 mV/s.

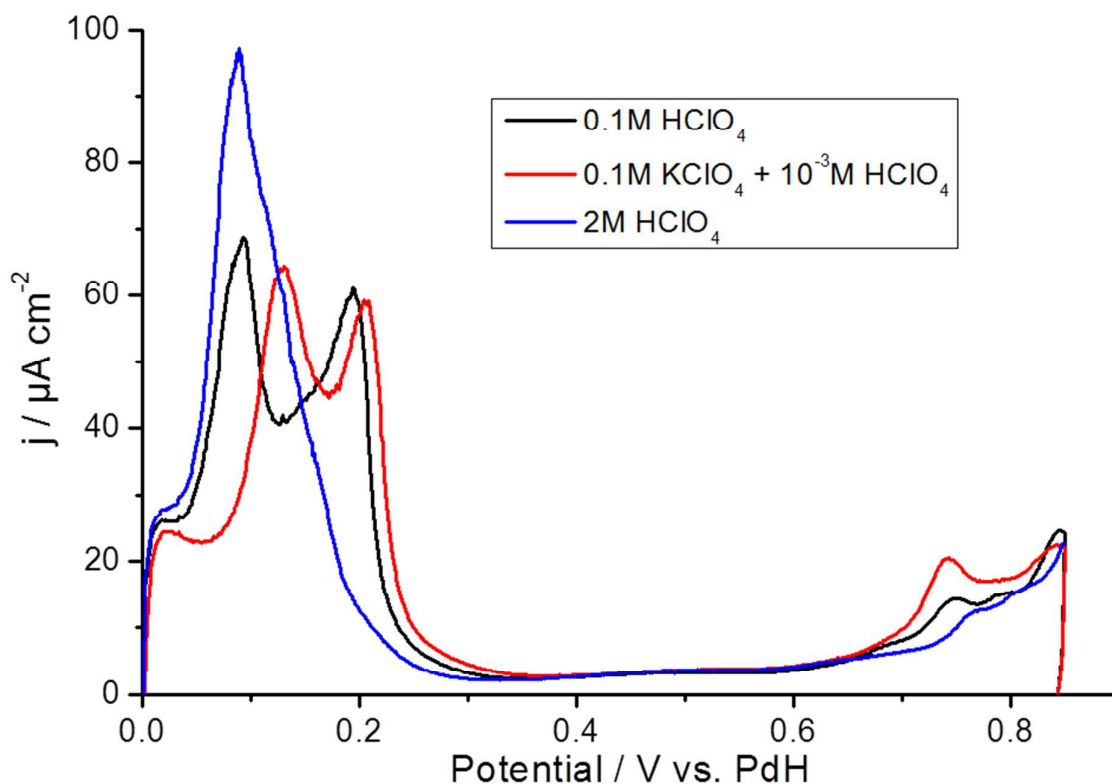


Figure 6 CV data for Pt{110} as a function of aqueous perchloric acid concentration and pH. Sweep rate = 50 mV/s.

However, in contrast to Pt{100}, figures 5 and 6 seem to show some inhibition of electrochemical oxide formation between 0.7 and 0.9 V as perchloric acid concentration is increased although no potential shift in the large oxide peak at 0.96 V is ever observed. This weak inhibition of the onset of oxide formation may be mimicked by spiking the perchloric acid electrolyte with sulphuric acid (figure 7) whereby a shift of the small oxide peak at 0.74 V can be induced even at 10^{-5} M sulphate concentration. As expected, addition of specifically adsorbing sulphate anions also causes a marked shift to more negative potentials of the H UPD state at 0.22 V to 0.11 V. In this context, the shift to more negative potentials of the 0.22V peak with increasing perchloric acid concentration seems to imitate the action of adding sulphate anions. However, in one respect it differs markedly. It is found that instead of merely transferring electroadsorption charge from the 0.22 V feature into the 0.09 V peak, specifically adsorbed sulphate acts exclusively on the charge associated with the 0.22V peak and does not in any way increase the intensity of the 0.09 V peak. Again, since sulphate clearly specifically adsorbs more strongly than perchlorate, why should sulphate not cause a

more negative shift in H UPD charge from the state at 0.22 V (i.e. why does the sulphate induced H UPD peak not appear at potentials negative of 0.09 V?).

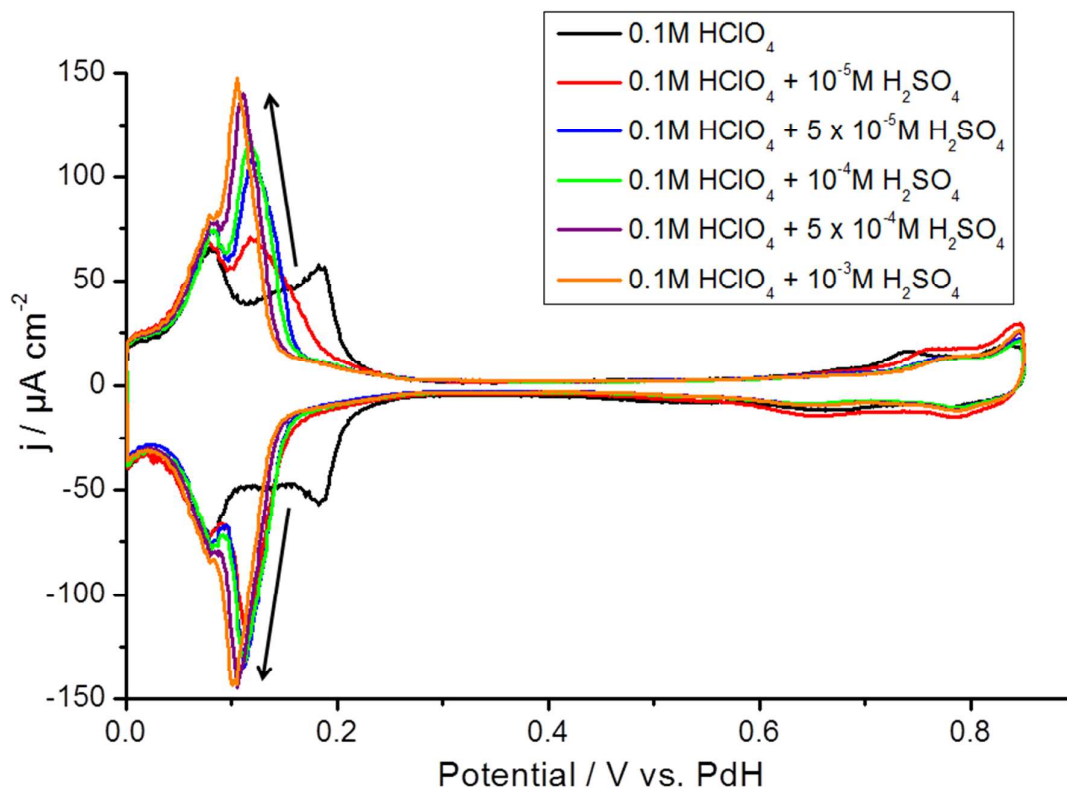


Figure 7 CV data for Pt{110} in 0.1 M aqueous perchloric acid as a function of increasing sulphuric acid concentration. Sweep rate = 50 mV/s.

We conclude in fact that, as for Pt{100}, the changes induced in the H UPD region are largely the result of changes in pH. Clearly (as for Pt{100} H UPD states), the nature of the H UPD peak at more negative potentials is quite different to the peak at more positive potentials, based on pH changes and behaviour exhibited towards specific adsorption. Hence, we conclude that for Pt{110} the majority of changes in the H UPD region as perchloric acid concentration is increased may be ascribed to pH effects although some perturbation of initial electrochemical oxide phase formation suggests specific adsorption of perchlorate may be causing this effect.

3.1.4 Pt{311}

In order to examine the influence of steps on the likelihood of specific adsorption by perchlorate anions, a Pt{311} (Pt 2{111}x{100}) electrode was examined. Figure 8 shows the CV response of Pt{311} in 0.1 M and 2M perchloric acid. In 0.1 M perchloric acid, three distinct H UPD states at 0.07, 0.24 and 0.32 V are identified. Of these, the peak at 0.07 V remains unchanged in potential and magnitude upon increasing perchloric acid concentration to 2M. Similarly, the 0.24 V peak shifts to more negative potentials by 11 mV whereas the 0.32 V peak shifts by 44 mV when acid concentration is increased causing appreciable overlap of these two peaks. The magnitudes of changes in peak potentials are commensurate with those reported for Pt{110} and we suggest a similar underlying mechanism. Namely, that for zero or small change in H UPD peak potential as pH decreases, the important surface process occurring is proton electrosorption. However, for the 0.32 V peak, a process of H replacement by OH-type species would rationalise the shift⁶⁸. Interestingly, it is the same H UPD peaks (those at more positive potentials) that are strongly perturbed by Nafion, adsorbed on Pt{hkl} compared to the states lying more negative of the pztc of the surface⁵⁷. The possible nature of the OH-type species being perturbed by the Nafion layer was also discussed in reference⁵⁷ and the link with pztc would in the present study also rationalise why the peaks at most negative potentials are hardly changed by anions (either OH, perchlorate or sulphate) because such peaks lie negative of the pztc thus inhibiting anion adsorption. Modest changes in the CV of Pt{311} in the range of electrochemical oxide formation are observed upon increasing perchloric acid concentration from 0.1 M to 2 M. In particular, the large peak at 0.9 V is seen to narrow with loss of intensity from the small shoulder at 0.86 V seen in 0.1 M acid and a new state appearing at 1 V. Again, we attribute such changes to weak specific adsorption of perchlorate.

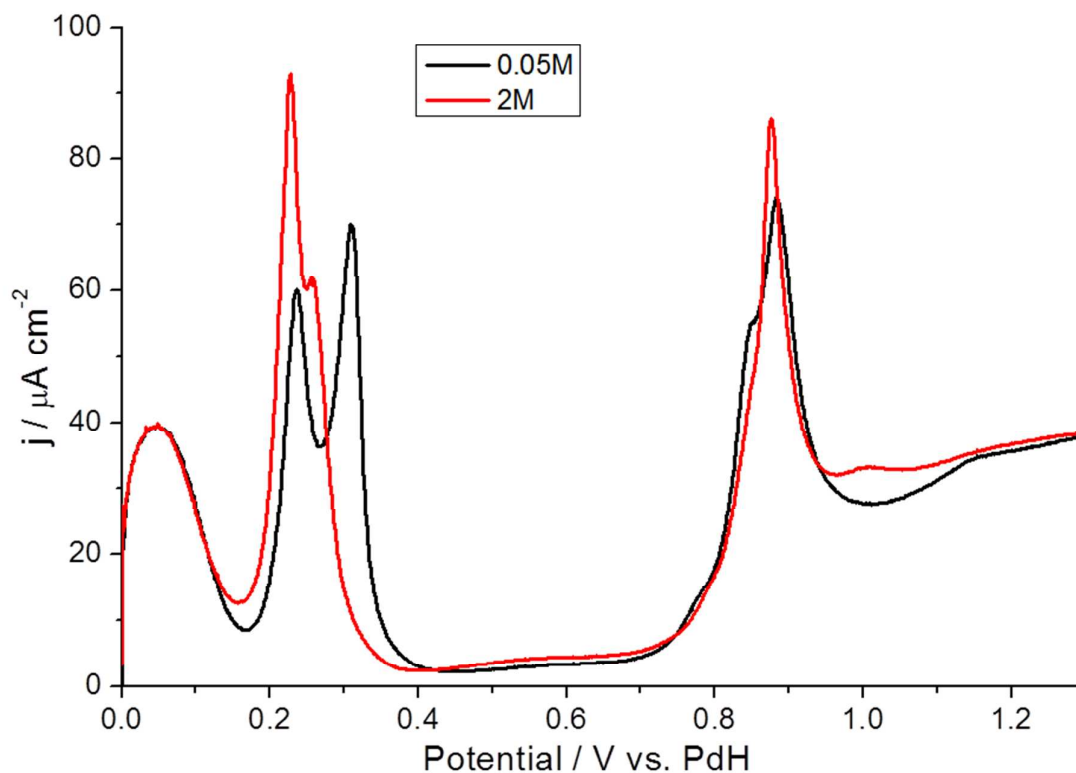


Figure 8 CV data for Pt{311} in 0.1 M and 2 M aqueous perchloric acid. Sweep rate = 50 mV/s.

It is interesting now to compare all of the perchloric acid results reported in sections 3.1.1 through 3.1.4 (especially the electrochemical oxide regions) with a recent paper by Feliu et al. in which the CVs of Pt{111}, Pt{100} and Pt{110} using 0.1 M perchloric acid aqueous electrolyte are compared with 0.1 M trifluoromethanesulphonic acid (TFMSA) aqueous electrolyte⁶⁹. In reference⁶⁹, the Pt-O peak (at 1 V) on Pt{111} is situated at more positive potentials in perchloric acid compared with TFMSA. We suggest that TFMSA is truly non-specifically adsorbed and it is weak specific adsorption of perchlorate causing this difference in potential of the Pt-O peak. Similarly, the small oxide peak at 0.74 V on Pt{110} referred to earlier, is found to occur at a more negative potential in TFMSA compared to perchloric acid. We suggest that this is further evidence that TFMSA is non-specifically adsorbed whereas perchlorate exhibits a weak specific adsorption on platinum. Finally, for Pt{100}, hardly any change in the Pt-O oxide peak is reported in reference⁶⁹ for the two electrolytes TFMSA and perchloric acid in agreement with our findings that Pt{100} exhibits the weakest interaction with perchlorate anions. Therefore, it is recommended that any electrocatalytic studies that

wish to eliminate the possibility of specific adsorption on platinum should use TFSA instead of perchloric acid. It is also interesting to note that according to work reported previously from the Frumkin School⁷⁰ that specific adsorption of anions is favoured as pH decreases. Hence, there is almost certainly a pH effect also being afforded in the present study in that as pH decreases, the actual interaction of perchlorate anion with the metal surface (if specifically adsorbed) should increase as seen for example in the case of Pt{111}.

3.2 Oxygen Reduction

The oxygen reduction reaction (ORR) has been shown in many studies to be sensitive to the presence of any anions in solution that may specifically adsorb on the surface of platinum^{11, 12, 15, 28, 29, 71}. On Pt{111}, (bi)sulphate adsorption from sulphuric acid solutions inhibits the ORR so that the half-wave potential ($E_{1/2}$) is ~ 200 mV more negative in potential than that observed in perchloric acid^{15, 17}. A similar effect has also been observed in phosphoric acid solutions due to the specifically adsorbing phosphate anion⁴¹. Bromide and chloride anions also cause an inhibition in the ORR due to their strong specific adsorption on Pt^{28, 29}. In order to emphasise correlations between ORR activity and specific adsorption, we show the behaviour exhibited by Pt{111} in a series of electrolytes (including different concentrations of perchloric acid) in relation to the onset of oxide formation (figure 9). As has been shown previously, specific adsorption of (bi)sulphate at potentials around 0.4 V in sulphuric acid protects this surface from oxidation such that the Pt-O peak appears at a rather positive (1.3V) potential compared to observations in perchloric acid (1V)⁵⁸. If the Pt-O peak can be used as a test for specific anion adsorption in this way, then comparing 0.1 M HClO₄ with 0.1 M NaOH reveals that ClO₄⁻ also specifically adsorbs (since the Pt-O peak is located at more positive potentials than in 0.1 M NaOH). Presumably, ClO₄⁻ adsorption “protects” the surface against oxidation to form Pt-O until higher potentials are reached (1.00 V) compared with NaOH (0.95 V). The specific adsorption of the sulphonate groups of Nafion^{56, 57} is also shown to affect the oxide peak of Pt{111} in perchloric acid by shifting Pt-O formation to 1.05 V. We also emphasise that the maximum value of current density for the “butterfly” peak (excluding sulphuric acid which does not involve OH_{ad}) also follows the exact same trend as for Pt-O as a function of electrolyte specific adsorption strength.

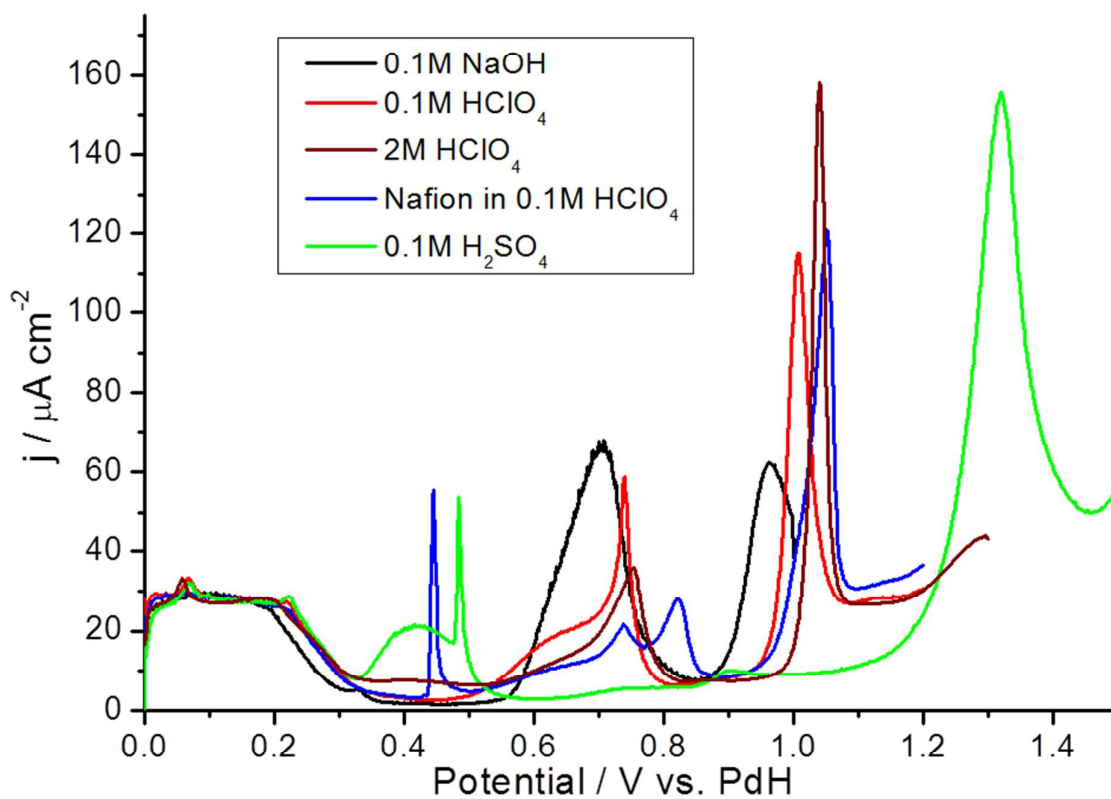


Figure 9 CV data for Pt{111} as a function of specific anion adsorption (positive going sweep) in various aqueous electrolytes. Sweep rate = 50 mV/s.

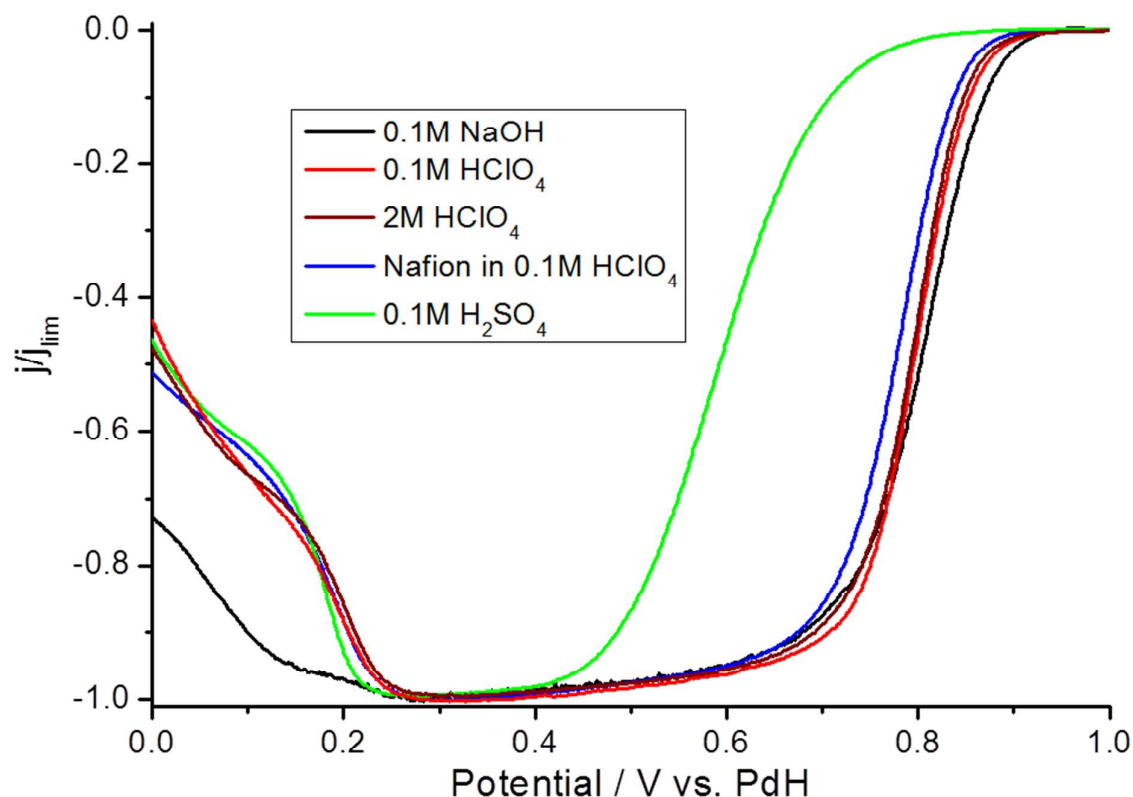


Figure 10 ORR data for Pt{111} in a hanging meniscus rotating disc electrode configuration (positive going sweep) in various aqueous electrolytes. Potential sweep rate = 30 mV/s. Rotation speed = 1600 rpm.

Figure 10 compares the ORR activity of Pt{111} in electrolytes with varying strengths of anion adsorption (based on the analysis above). ORR activity (as measured using a rotating disc electrode in a hanging meniscus configuration) in 0.1 M NaOH, 0.1 M HClO₄, 2 M HClO₄, 0.1 M HClO₄ with Nafion adsorbed, and 0.1 M H₂SO₄ are shown. In 0.1 M H₂SO₄ the activity of Pt{111} is very low, with an $E_{1/2}$ of ~600mV, in agreement with previous reports. The other solutions investigated in this study show ORR half-wave potentials clustered around 0.8V, with their exact order correlating well with the strength of anion adsorption discussed in figure 9. The ORR of Pt{111} in 0.1 M HClO₄ with adsorbed Nafion exhibits the second most negative $E_{1/2}$ value, followed by 2M HClO₄. The difference in activity for ORR between 2M and 0.1M perchloric acid electrolytes is very small, with the lower concentration resulting in a higher activity, presumably due to there being less specifically adsorbed perchlorate blocking the reduction of oxygen at lower concentrations of HClO₄. The highest activity is seen in 0.1 M NaOH, which presents an $E_{1/2}$ value slightly

more positive than 0.1M HClO₄ (Table 1). This suggests that the hydroxide anion specifically adsorbs less strongly than any other anions tested in figure 10. Therefore its inhibitory effect on the ORR is the lowest. We would predict that TFMSA electrolytes would also exhibit slightly greater ORR activity than 0.1 M perchloric acid.

Table 1 showing variation in ORR current density on Pt{111} as a function of specifically adsorbing anion.

| Surface/Solution | Current Density at 0.85V (mA cm ⁻²) |
|---|--|
| Pt{111} - 0.1M NaOH | 1.11 |
| Pt{111} - 0.1M HClO ₄ | 0.70 |
| Pt{111} - 2M HClO ₄ | 0.558 |
| Pt{111}/Nafion - 0.1M HClO ₄ | 0.36 |
| Pt{111} – 0.1M H ₂ SO ₄ | <0.025 |

4 Conclusion

The specific adsorption of perchlorate anions on Pt{hkl} has been investigated in acidic aqueous media together with ORR on Pt{111}. It is concluded that specific adsorption of perchlorate does take place on platinum in agreement with previous studies by Watanabe and co-workers^{36, 48, 52} and that the extent of this interaction follows the order:

$$\text{Pt}\{111\} > \text{Pt}\{311\} \geq \text{Pt}\{110\} > \text{Pt}\{100\}.$$

Significant changes in the H UPD region of all Pt{hkl} surfaces (except Pt{111}) when perchloric acid concentration is increased from 0.05 to 2 M are attributed to changes in solution pH. On Pt{111} perchlorate anion adsorption is found to inhibit ORR and so it is recommended that future investigations of any electrocatalytic behaviour on Pt (particularly ORR) should employ TFMSA rather than perchloric acid if specific adsorption effects are required to be eliminated.

Acknowledgements

GAA would like to thank both the EPSRC and Johnson Matthey for financial support and studentships for AB and KH.

References

1. F. T. Wagner, B. Lakshmanan and M. F. Mathias, *J. Phys. Chem. Lett.*, 2010, **1**, 2204-2219.
2. J. V. Mierlo, G. Maggetto and Ph. Lataire, *Energy Convers. Manage.*, 2006, **47**, 2748-2760.
3. R. H. Borgwardt, *Transportation Research Part D-Transport and Environment*, 2001, **6**, 199-207.
4. M. K. Debe, *Nature*, 2012, **486**, 43-51.
5. A. A. Gewirth and M. S. Thorum, *Inorg. Chem.*, 2010, **49**, 3557-3566.
6. M. Watanabe, D.A. Tryk, M. Wakisaka, H. Yano and H. Uchida, *Electrochim. Acta*, 2012, **84**, 187-201.
7. A. M. Gómez-Marín and J. M. Feliu, *ChemSusChem*, 2013, **6**, 1091-1100.
8. W. Yu, M. D. Porosoff and J. G. Chen, *Chem. Rev.*, 2012, **112**, 5780-5817.
9. D. van der Vliet, C. Wang, M. Debe, R. Atanasoski, N. M. Markovic and V. R Stamenkovic, *Electrochim. Acta*, 2011, **56**, 8695-8699.
10. J. K. Nørskov, J. Rossmeisl, A. Logadottir, L. Lindqvist, *J. Phys. Chem. B*, 2004, **108**, 17886-17892.
11. A. Kuzume, E. Herrero and J. M. Feliu, *J. Electroanal. Chem.*, 2007, **599**, 333-343.
12. M.D. Maciá, J.M. Campiña, E. Herrero and J. M. Feliu, *J. Electroanal. Chem.*, 2004, **564**, 141-150.
13. R. Rizo, E. Herrero and J. M. Feliu, *Phys. Chem. Chem. Phys.*, 2013, **15**, 15416-15425.
14. V. R. Stamenkovic, B. S. Mun, M. Arenz, K. J. J. Mayrhofer, C. A. Lucas, G. Wang, P. N. Ross and N. M. Markovic, *Nat. Mater.*, 2007, **6**, 241-247.
15. N. M. Marković, H. A. Gasteiger and P. N. Ross, *J. Phys. Chem.*, 1995, **99**, 3411-3415.
16. N. M. Marković, H. A. Gasteiger and P. N. Ross, *J. Phys. Chem.*, 1996, **100**, 6715-6721.
17. N. M. Marković, R. R. Adžić, B. D. Cahan and E. B. Yeager, *J. Electroanal. Chem.*, 1994, **377**, 249-259.
18. V. Climent and J. M. Feliu, *J. Solid State Electrochem.*, 2011, **15**, 1297-1315.
19. Y. Liu, C. M. Hangarter, U. Bertocci and T. P. Moffat, *J. Phys. Chem. C*, 2012, **116**, 7848-7862.
20. I. E. L. Stephens, A. S. Bondarenko, F. J. Perez-Alonso, F. Calle-Vallejo, L. Bech, T. P. Johansson, A. K. Jepsen, R. Frydendal, B. P. Knudsen, J. Rossmeisl and I. Chorkendorff, *J. Am. Chem. Soc.*, 2011, **133**, 5485-5491.
21. G. A. Attard, J. Ye, A. Brew, D. Morgan, P. Bergstrom-Mann and S. Sun, *J. Electroanal. Chem.*, 2013.
22. S.-M. Hwang, C. H. Lee, J. J. Kim and T. P. Moffat, *Electrochim. Acta*, 2010, **55**, 8938-8946.
23. V. Stamenkovic, B. Fowler, B. S. Mun, G. Wang, P. N. Ross, C. A. Lucas and N. M. Marković, *Science*, 2007, **315**, 493-497.
24. N. M. Marković, T. J. Schmidt, V. Stamenković and P. N. Ross, *Fuel Cells*, 2001, **1**, 105-116.
25. T. Yu, D. Y. Kim, H. Zhang and Y. Xia, *Angew. Chem., Int. Ed.*, 2011, **50**, 2773-2777.
26. N. M. Marković, N. S. Marinković and R. R. Adžić, *J. Electroanal. Chem. Interfacial Electrochem.*, 1988, **241**, 309-328.
27. N. M. Marković, N. S. Marinković and R. R. Adžić, *J. Electroanal. Chem. Interfacial Electrochem.*, 1991, **314**, 289-306.
28. V. Stamenkovic, N. M. Markovic and P. N. Ross, *J. Electroanal. Chem.*, 2001, **500**, 44-51.
29. N. M. Markovic, H. A. Gasteiger, B. N. Grgur and P. N. Ross, *J. Electroanal. Chem.*, 1999, **467**, 157-163.
30. V. Lazarescu, J. Clavilier, *Electrochim. Acta*, 1998, **44**, 931-941.
31. K. A. Jaaf-Golze, D. M. Kolb and D. Scherson, *J. Electroanal. Chem. Interfacial Electrochem.*, 1986, **200**, 353-362.
32. J. Clavilier, R. Albalat, *J. Electroanal. Chem.*, 1992, **330**, 489-497.

33. F. T. Wagner and P. N. Ross, *J. Electroanal. Chem. Interfacial Electrochem.*, 1998, **250**, 301-320.
34. M. Teliska, V. S. Murthi, S. Mukerjee and D. E. Ramaker, *J. Phys. Chem. C*, 2007, **111**, 9267-9274.
35. K. Kunitatsu, H. Hanawa, H. Uchida and M. Watanabe, *J. Electroanal. Chem.*, 2009, **632**, 109-119.
36. H. Uchida, H. Ozuka and M. Watanabe, *Electrochim. Acta*, 2002, **47**, 3629-3636.
37. J. Mostany, E. Herrero, J. M. Feliu and J. Lipkowsky, *J. Phys. Chem. B*, 2002, **106**, 12787-12796.
38. G. A. Attard, J. Ye, P. Jenkins, F. J. Vidal-Iglesias, E. Herrero, S. Sun, *J. Electroanal. Chem.*, 2013, **688**, 249-256.
39. N. Garcia-Araez, V. Climent, E. Herrero, J. M. Feliu and J. Lipkowsky, *J. Electroanal. Chem.*, 2005, **576**, 33-41.
40. J. Mostany, P. Martinez, V. Climent, E. Herrero and J. M. Feliu, *Electrochim. Acta*, 2009, **54**, 5836-5843.
41. Q. He, X. Yang, W. Chen, S. Mukerjee, B. Koel and S. Chen, *Phys. Chem. Chem. Phys.*, 2010, **12**, 12544-12555.
42. A. Rodes, E. Pastor and T. Iwasita, *J. Electroanal. Chem.*, 1994, **376**, 109-118.
43. J. K. Norskov, J. Rossmeisl, A. Logadottir, L. Lindqvist, J. R. Kitchin, T. Bligaard and H. Jonsson, *J. Phys. Chem. B*, 2004, **108**, 17886-17892.
44. J. Zhang, M. B. Vukmirovic, Y. Xu, M. Mavrikakis and R. R. Adzic, *Angew. Chem., Int. Ed.*, 2005, **44**, 2132-2135.
45. V. R. Stamenkovic, B. Fowler, B. S. Mun, G. Wang, P. N. Ross, C. A. Lucas and N. M. Markovic, *Science*, 2007, **315**, 493-497.
46. C. Cui, L. Gan, M. Heggen, S. Rudi and P. Strasser, *Nat. Mater.*, 2013, **12**, 765-771.
47. H. R. Colon Mercado and B. N. Popov, *J. Power Sources*, 2006, **155**, 253-263.
48. G. Horányi and I. Bakos, *J. Electroanal. Chem.*, 1992, **331**, 727-737.
49. G. G. Lang, N. S. Sas, M. Ujvári and G. Horányi, *Electrochim. Acta*, 2008, **53**, 7436-7444.
50. A. Ahmadi, R. W. Evans and G. A. Attard, *J. Electroanal. Chem.*, 1993, **350**, 279-295.
51. M. Yu, P. Polásková, M. Muzikar and W. R. Fawcett, *Electrochim. Acta*, 2006, **51**, 3097-3101.
52. G. G. Láng and G. Horányi, *J. Electroanal. Chem.*, 2003, **552**, 197-211.
53. J. Clavilier, R. Faure, G. Guinet and R. Durand, *J. Electroanal. Chem.*, 1980, **107**, 205-209.
54. N. Markovic, M. Hanson, G. McDougall and E. Yeager, *J. Electroanal. Chem. Interfacial Electrochem.*, 1986, **214**, 555-566.
55. B. D. Cahan and H. M. Villullas, *J. Electroanal. Chem.*, 1991, **307**, 263-268.
56. R. Subbaraman, D. Strmcnik, V. Stamenkovic and N. M. Markovic, *J. Phys. Chem. C*, 2010, **114**, 8414-8422.
57. M. Ahmed, D. Morgan, G. A. Attard, E. Wright, D. Thompsett and J. Sharman, *J. Phys. Chem. C*, 2011, **115**, 17020-17027.
58. A. Bjorling, E. Herrero, J. M. Feliu, *J. Phys. Chem. C*, 2011, **115**, 15509-15515.
59. A. Berná, V. Climent and J. M. Feliu, *Electrochem. Commun.*, 2007, **9**, 2789-2794.
60. Y. Sawatari, J. Inukai and M. Ito, *J. Electron Spectrosc. Relat. Phenom.*, 1993, **64-65**, 515-522.
61. K. Hirota, M. Song and M. Ito, *Chem. Phys. Lett.*, 1996, **250**, 335-341.
62. A. Rodes, M. A. Zamakhchari, K. El Achi and J. Clavilier, *J. Electroanal. Chem. Interfacial Electrochem.*, 1991, **305**, 115-129.
63. A. Rodes, J. Clavilier, J. M. Orts, J. M. Feliu and A. Aldaz, *J. Electroanal. Chem.*, 1992, **338**, 317-338.
64. V. Climent, R. Gómez, J. M. Orts and J. M. Feliu, *J. Phys. Chem. B*, 2006, **110**, 11344-11351.
65. M. E. Gamboa-Aldeco, E. Herrero, P. S. Zelenay and A. Wieckowski, *J. Electroanal. Chem.*, 1993, **348**, 451-457.
66. N. Garcia-Araez, V. Climent, J. M. Feliu, *J. Phys. Chem. C*, 2009, **113**, 9290-9304.
67. D. J. Schmidt, W. Chen, C. Wolverton and W. F. Schneider, *J. Chem. Theory Comput.*, 2012, **8**, 264-273

68. M. van der Niet, N. Garcia-Areaz, J. Hernandez, J. M. Feliu, M. Koper, *Catal. Today*, 2013, **202**, 105-113.
69. A. Berná, J. M. Feliu, L. Gancs and S. Mukerjee, *Electrochem. Commun.*, 2008, **10**, 1695-1698.
70. A.N. Frumkin, O.A. Petrii and B.B. Damaskin, *Comprehensive Treatise of Electrochemistry*, Volume 1, Ed. J. O'M. Bockris, B.E. Conway and E. Yeager, Plenum, New York, 1980.
71. D. Strmcnik, M. Escudero-Escribano, K. Kodama, V. R. Stamenkovic, A. Cuesta and N. M. Markovic, *Nat. Chem.*, 2010, **2**, 880-885.